COO-4012-72

Physica Scripta. Vol. T5, 175–177, 1983.

Transition from Prolate to Oblate to Triaxial Shapes in ^{158}Yb

M. Jääskeläinen,* D. G. Sarantites, F. A. Dilmanian, R. Woodward and H. Puchta†

Department of Chemistry, Washington University, St. Louis, MO 63130, U.S.A.

and

J. R. Beene, J. Hattula,* M. L. Halbert and D. C. Hensley

Oak Ridge National Laboratory, Oak Ridge, TN 37830, U.S.A.

Received October 13, 1982; accepted November 19, 1982

Abstract

The decay of the entry states in ^{158}Yb populated in the reactions of 149 MeV ^{20}Ne with ^{144}Nd and ^{146}Nd has been investigated with a 4π multidetector system gated by a Ge counter. The average excitation energy, the γ-ray spectra and the angular distributions as a function of multiplicity show several changes in the γ-ray decay. These changes suggest a transition from prolate to particle aligned oblate configuration at low spin. At $I \sim 38$–48 collective transitions with dipole and quadrupole component possibly built on high K single particle states are observed. Furthermore, above $I \sim 48$ the dipole component disappears suggesting a further change toward more triaxial shape.

1. Introduction

The evolution of nuclear shapes as a result of the interplay of the single particle and collective degrees of freedom has been the subject of intensive theoretical and experimental investigation in the past few years [1–3]. Experimentally only a few nuclei has been found to obtain an oblate ground state. With increasing angular momentum, however, an alignment of quasi-particle angular momenta tends to make the nucleus oblate. The nuclei around $A = 150$ are known to have few-particle yrast states up to $I \simeq 38$ with a small oblate deformation ($\epsilon \sim 0.1$–0.2) [4]. This behaviour is well understood also with the rotating liquid drop model [5], which predicts the evolution of nuclear shapes with increasing angular momentum from spherical, at $I = 0$, to increasingly deformed oblate structure up to $I \sim 70$ (for $A = 160$). This behaviour is, however, expected to be strongly modified by the shell structure of the nuclei.

For nuclei $A \sim 160$ the shell effects at low spins cause the significant prolate deformations ($\epsilon \sim 0.2$–0.3) observed. The excitation energy and angular momentum are then generated by collective rotation around an axis perpendicular to the symmetry axis. However, with increasing rotational frequency, the pairing can be broken and a few particles align their spin vectors along the rotation axis. These effects cause the back-bending phenomenon [3] and can break the axial symmetry, but the nuclei retain basically prolate shape ($\gamma \simeq 0°$) [6]. Alignment of additional particles and the rotation can increase the shell energy for prolate shape and finally lead to an oblate nucleus rotating around the symmetry axis. Thus the tendency for prolate nuclei to become oblate with increasing angular momentum is a combined liquid drop and shell effect. For nuclei with $N > 90$ the negative shell energy for prolate shape is so strong that a transition from prolate to oblate shape is not likely [7]. The good rotational behaviour of those nuclei is also experimentally [3] observed up to spin $\sim 65\,\hbar$. Thus the nuclei with $N \simeq 85$–90 on the border of the deformation region are the most probable candidates for such a change.

Transitions from one type of behaviour to another may be observable in a single nucleus as a function of I. For example, recent evidence suggests that collectivity in ^{152}Dy may set in above $I = 30$ [8], that a change may occur in ^{154}Dy at $I \sim 30$ from prolate to oblate via triaxial shapes [9], and that a transition from prolate to a collectively rotating oblate shape appears to take place in ^{160}Yb at $I \simeq 45$ [10]. In view of this evidence and the prediction of super-deformed configurations ($\epsilon \sim 0.6$) in $N \sim 86$ nuclei [11], it seemed that ^{158}Yb ($N = 88$) would be a good candidate for studying the evolution of nuclear shape as a function of spin.

2. Experimental methods

Metallic targets of ^{144}Nd and ^{146}Nd were bombarded with 149 MeV ^{20}Ne beams from ORIC. The triggering signal for the electronics of the Spin Spectrometer, a 4π multidetector system, was derived from a Ge detector positioned at 117° to the beam. In the data analysis the exit channels were selected by gating on known low lying gamma transitions in ^{158}Yb. In these experiments 69 out of 72 NaI detectors (92.3% of 4π) in the spectrometer were used. For each event the Ge pulse height and its time relative to the cyclotron RF and all nonzero pulse heights from the NaI detectors and their times relative to the Ge trigger were recorded. The event tapes were first processed to correct for nonlinearities in the NaI pulse heights, match the gains of the NaI elements, derive an accurate reference time for each event by averaging the times of the NaI γ-pulses, and separate neutron and γ-ray pulses by time of flight. The processed events were then sorted to construct the desired spectra.

2.1. *Entry state measurements*

The final events were used to get the population of ^{158}Yb for each γ-ray coincidence fold (k) and each 1.0 MeV interval in total γ-ray pulse height (H). Gates on the 358 keV 2^+–0^+ transition and nearby background were placed on the Ge pulse height and the events scanned to produce the $Q_X(H, k)$ distributions. The entry state populations, $R_X(E^*, M_\gamma)$, in exitation energy-multiplicity space were obtained from the measured distributions $Q_X(H, k)$ by an iterative least-squares unfolding

* Present address: Department of Physics, University of Jyväskylä, Jyväskylä, Finland.
† Present address: Department of Physics, University of Munich, Munich, West Germany.

procedure [12]. Some of the angular momentum and exitation energy is removed by low energy or delayed transitions (below the gating transition) that were not detected by the spectrometer. The M_γ and E^* distributions for these channels have been shifted to compensate for these undetected transitions [13]. The response functions of the spectrometer, $P(E^*, M_\gamma \to H, k)$, used in the unfolding procedure were constructed from data taken with radioactive sources as described in [12].

2.2. *Gamma-ray decay measurements*

The γ-ray decay of the entry states was studied using the NaI detectors in the spectrometer. The pulse height spectra for each coincidence fold, k, were constructed from five different groups of detectors at angles of 24.4°, 45.6°, 65.7°, 77.5° and 87.3° (and their supplements) with respect to the beam. These spectra were constructed in coincidence with the 2^+–0^+ yrast transition observed in the Ge detector and corrected for the underlying Compton background in the Ge gate. The NaI pulse height spectra were then unfolded to yield the γ-ray energy spectra by an iterative unfolding procedure that corrects for the responses of the detectors. These were obtained from measurements with radioactive sources of γ-ray energies between 136 keV and 4439 keV and included the effects of detector to detector scattering and coicidence summing appropriate for each pulse height spectrum [12]. The associated multiplicities for each spectrum (or coincidence fold) were determined from the spectrometer response functions, $P(E^*, M_\gamma \to H, k)$, and the deduced entry state populations, $R_X(E^*, M_\gamma)$, as described in detail in [12]. The γ-decay of the entry states was investigated for $M = 7$ to 22 for ^{146}Nd(^{20}Ne, 8n) and $M = 12$ to 30 for ^{144}Nd(^{20}Ne, 6n) reaction.

3. Experimental results

The observed entry lines $\langle E^* \rangle$ vs. multiplicity for both reactions are shown in Fig. 1. The entry lines show four different slopes as a function of multiplicity. As seen from Fig. 1, the slope increases slightly at $M \approx 16$, decreases sharply at $M_\gamma \approx 22$ and finally increases again at $M_\gamma \approx 28$. These changes of the slopes of the entry lines $\langle E^* \rangle$ vs. M_γ are associated with changes in the γ-ray spectra associated with each multiplicity. Thus changes in the nuclear structure as a function of spin in ^{158}Yb are obvious. Selected energy spectra from the 8n reaction, obtained from all the NaI detectors in the spectrometer and normalized to their respective multiplicities are shown in Fig. 2(a). They correspond to selected single k values. Spectra from the 6n reaction corresponding to bins of three consecutive k values are shown in Fig. 2(b). The labels in Fig. 2 are the mean values of M_γ corresponding to each k-bin. The six k gates for the 6n reaction correspond to the M_γ regions shown in Fig. 1. The sharp edges may be deceptive, as the M_γ gates actually extend about 2 units above and below the indicated ranges due to the finite M_γ resolution of the spectrometer.

The yrast decay scheme of ^{158}Yb is known up to $I = 12$ and consists of a cascade of stretched E2 transitions, with E_γ from 358 to 683 keV [14]. The behaviour of the observed γ-ray spectrum is consistent with a continuation of a predominantly quadrupole cascade at least up to $M_\gamma \approx 15$. The angular distribution of the γ-rays for M_γ between 14 and 20 are less anisotropic than would be expected for pure quadrupole radiation. Moreover at $M_\gamma \approx 16$–20 the additional contribution to the γ-ray spectra with increasing M_γ, occur not only at the high

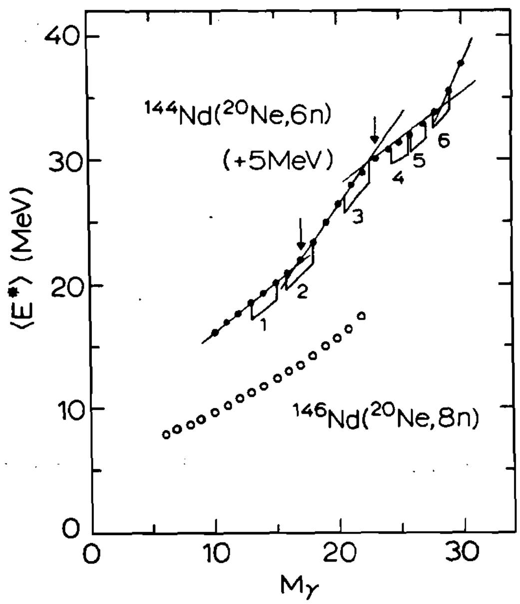

Fig. 1. Entry lines, E^* vs. M_γ. The data points are from the reactions indicated. The data for the ^{144}Nd target is shifted by + 5 MeV. The solid lines indicate the four different slope as a guide to the eye. The bracketed regions marked 1 to 6 give the M_γ gates used for the γ-ray spectra in Fig. 2(b). The vertical arrows mark the changing points in the entry line.

E_γ edge but almost equally between 0.5–1.0 MeV as seen from Fig. 2. This observation suggest a tendency toward non-collective transitions, which in the lighter rare earth nuclei have been associated with aligned quasiparticle structure with small oblate deformation [1].

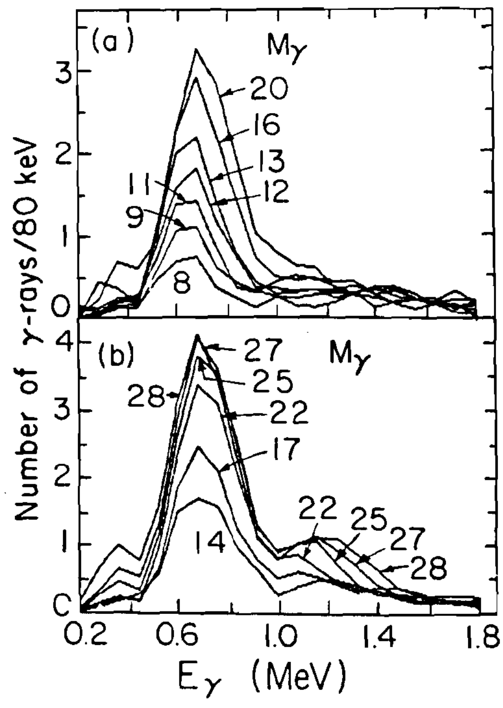

Fig. 2. (a) Unfolded γ-ray continuum spectra for single-k bins normalized to the associated M_γ from the ^{146}Nd(^{20}Ne, 8n) reaction. (b) Unfolded γ-ray continuum spectra from k-bins of three consecutive k values normalized to M_γ. These spectra correspond to the M_γ gates bracketed in Fig. 1.

A different behaviour is seen at higher M_γ. Above $M_\gamma \simeq 22$ the additional γ-rays are localized into two separate components. Related effects are observed in the entry line and in the angular distributions. At $M_\gamma \simeq 22$ the entry line (Fig. 1) begins to bend down significantly. In the same M_γ region the lower half ($E_\gamma \sim 700$ keV) of the spectrum develops an angular distribution characteristic of stretched dipole radiation. All three observations are consistent with the onset at $M_\gamma \simeq 22$ of a strong dipole component which is well localized in E_γ. From the spectra at various angles, we estimate that the dipole energies are confined to a narrow energy region at ~ 650 keV with a full width half maximum of ~ 200 keV.

For $M_\gamma \gg 22$ the high energy bump becomes increasingly prominent. This bump evolves up to the highest M_γ in just the way expected for a rotational quadrupole cascade with approximately constant moment of inertia. The angular distribution data show clearly that the transitions in this energy region are consistent with stretched E2.

Another change in decay mode at high M_γ is apparent in Fig. 2(b). The dipole component at $E_\gamma \sim 650$ keV stops increasing at $M_\gamma \simeq 27$. This is entirely consistent with the behaviour of the entry line (Fig. 1) which shows an upbend at this M_γ. Above $M_\gamma = 28$ the entry line has resumed the slope expected for predominantly quadrupole cascades.

To summarize our experimental observations, the continuum spectroscopy of ^{158}Yb can be divided into three, or perhaps four, angular momentum regions with distinctive characteristics. At low spin ($I \leq 25$) ^{158}Yb is known to be a prolate rotor. At moderate spins ($I \sim 25$–38) there is evidence for noncollective effects in the continuum. At $I \simeq 38$ ($M_\gamma \simeq 22$) a dramatic change occurs. A strong stretched dipole component appears at an energy ($E_\gamma \simeq 650$ keV) one half the quadrupole edge at the same spin. These dipoles account for 50–60% of the additional transitions between $I = 38$ and 48. Nevertheless a stretched quadrupole component continues to evolve over this spin range in the way expected of a rotational spectrum. $I \simeq 48$ is another transition point. Above this spin no additional stretched dipole transitions were seen.

The observed evolution of the decay modes in ^{158}Yb can be related to the evolution in nuclear structure of the yrast states predicted by Bengtsson et al. [2]. These cranked modified oscillator calculations predict a prolate ground state for ^{160}Yb and ^{162}Yb. These nuclei are then predicted to become oblate at $I \approx 45$ ($A = 160$) and $I \approx 55$ ($A = 162$). These calculations, which do not include pairing, predict ^{158}Yb to be oblate even in its ground state. However, if the pairing is included the ground state of ^{158}Yb is prolate [15]. Above $I \simeq 30$ and $I \simeq 45$, respectively, ^{158}Yb and ^{160}Yb are predicted to evolve toward increasing oblate deformation with increasing spin until triaxial shapes with rapidly increasing deformations become favored at spin 60 and 70$\hbar$, respectively. The non-collective behaviour observed in our data between $I \simeq 28$ and 38 is consistent with the predicted transition to oblate shape at fairly low spin in ^{158}Yb. An oblate nucleus with not too large a deformation should have a non-collective, aligned quasiparticle spectrum [1, 2, 4]. It is possible that the region of strong dipole transitions is also associated with an oblate shape. The yrast states in an oblate nucleus are expected to be aligned ($K \simeq I$) quasiparticle states. If the deformation is sufficiently large the states could have rotational states built upon them [16]. Such high K bands are good candidates for producing M1 radiation since for intra-band transitions in the rotational model [14, 15], $B(\mathrm{M1}) \propto K^2$, while ($B(\mathrm{E2}) \propto 1/K$). The remarkable localization of dipole radiation at half the quadrupole energies supports the intra-band M1 speculation.

It is tempting to associate the disappearance of the dipole radiation above $I \sim 49$ with the predicted tendency of ^{158}Yb to move away from oblate shapes toward triaxiality near this spin. However, neither the experimental data nor the theoretical expectations are yet sufficiently well developed to clearly support such a suggestion.

Similar data also exist on ^{160}Yb [10]. The difference between ^{158}Yb and ^{160}Yb are in qualitative agreement with the calculation by Bengtsson et al. [2]. A similar stretched dipole component appears at $I \approx 45$, but additional stretched dipole transitions are seen up to the highest spin observed. There is no evidence for a non-collective region in ^{160}Yb, but the transition from prolate rotational quadrupole decay to high-K bands occur directly.

In summary four different decay modes which are reflected in continuum γ-ray spectra, multipole character of the γ-rays and the entry lines are observed in ^{158}Yb with increasing spin. These characteristics are qualitatively consistent with the evolution of nuclear shape with spin as predicted by the calculations of Bengtsson et al. [2].

Acknowledgements

This work was supported in part by U.S. Department of Energy. Oak Ridge National Laboratory is operated by Union Carbide Corporation for the U.S. Department of Energy under Contract No. W-745, eng.-26.

References

1. Bohr, A. and Mottelson, B. R., Phys. Scripta 10A, 13 (1974).
2. Bengtsson, R., Larsson, S. E., Leander, G., Möller, P., Nilsson, S. G., Aberg, S. and Szymanski, Z., Phys. Lett. 57B, 301 (1975).
3. Diamond, R. M. and Stephens, F. S., Ann. Rev. Nucl. Sci. 30, 85 (1980).
4. Khoo, T. L., Smither, R. R., Haas, B., Häusser, O., Andrews, H. R., Horn, D. and Ward, D., Phys. Rev. Lett. 41, 1022 (1978).
5. Cohen, S., Plasil, F. and Swiatechi, W. J., Ann. Phys. 82, 5 (1974).
6. Riedinger, L. L., Proc. of Nuclear Physics Workshop, Trieste (1981).
7. Ragnarson, I., Bengtsson, T., Leander, G. and Aberg, S., Nucl. Phys. A347, 287 (1980).
8. Chowdhury, P., Borggreen, J., Khoo, T. L., Ahmad, I., Smither, R. R., Faber, S. R., Daly, P. S., Dors, C. L. and Wilson, J., Phys. Rev. Lett. 47, 118 (1981).
9. Pakkanen, A., Chung, Y. H., Daly, P. J., Faber, S. R., Helppi, H., Wilson, J., Chowdhury, P., Khoo, T. L., Ahmad, I., Borggreen, J., Grabowski, Z. W. and Radford, D. C., Phys. Rev. Lett. 48, 1530 (1982).
10. Jääskeläinen, M., Sarantites, D. G., Woodward, R., Dilmanian, F. A., Puchta, H., Beene, J. R., Hattula, J., Halbert, M. L., Hensley, D. C. and Barker, J. H., Phys. Rev. Lett. 49, 1387 (1982).
11. Aberg, S., Larsson, S. E., Möller, P., Nilsson, S. G., Leander, G. and Ragnarsson, I., Physics and Chemistry of Fission 1979, Vol. I. IAEA Vienna (1980).
12. Jääskeläinen, M., Sarantites, D. G., Woodward, R., Dilmanian, F. A., Hood, S. T., Jääskeläinen, R., Hensley, D. C., Halbert, M. L. and Barker, J. H., Nucl. Instr. Meth. 204, 385 (1983).
13. Sarantites, D. G., Jääskeläinen, M., Woodward, R., Dilmanian, F. A., Hensley, D. C., Barker, J. H., Beene, J. R., Halbert, M. L. and Milner, W. T., Phys. Lett. 115B, 441 (1982).
14. Troutman, W., Proetel, D., Häusser, O., Hering, W. and Riess, F., Phys. Rev. Lett. 35, 1694 (1975).
15. Aberg, S., Phys. Scripta 25, 23 (1982).
16. Andersson, C. G., Krumlinde, J., Leander, G. and Szymanski, Z., Nucl. Phys. A361, 147 (1981).